Moisture Diffusion in Cementitious Materials

Adsorption Isotherms

Yunping Xi, Zdeněk P. Bažant, and Hamlin M. Jennings
Department of Civil Engineering, Northwestern University, Evanston, Illinois

This article describes an improvement on a previous model proposed by Bažant and Najjar, in which moisture diffusivity and moisture capacity are treated as separate parameters. These parameters are evaluated from independent test results, and are shown to depend on the water:cement ratio, curing time, temperature, and cement type. The moisture capacity is obtained as the slope of the adsorption isotherm. A mathematical model is developed and is shown to predict experimental adsorption isotherms of Portland cement paste very well. In the present form, the model is not applicable to high temperatures. ADVANCED CEMENT BASED MATERIALS 1994, 1, 248–257

T he properties of cementitious materials depend strongly on the moisture content. Therefore, knowledge of the moisture distribution within concrete structures at various times is of considerable practical importance. This is especially true if time-dependent phenomena such as creep, shrinkage, fire resistance, and durability are analyzed. The migration of moisture within concrete is more complex then in most other porous media because a very wide range of pore sizes is present in cement paste, and the pore structure changes with age. An accurate and general theoretical model for cementitious materials does not yet exist.

A very general model is that proposed by Bažant and Najjar [1]. It is used widely for diffusion analysis and, especially in computer programs, for predicting diffusion through nuclear containment and pressure vessels. This model involves an S-shaped curve that describes the dependence of the diffusion coefficient on the relative humidity within the pores in concrete, and, in a later extension by Bažant and Thonguthai [2]

and Bažant and Wittmann [3], also on the temperature and age of concrete.

However, the effects of composition, particularly the water:cement ratio, are not considered. The slope of the desorption isotherm, called moisture capacity, is assumed to be constant, although actually it is not constant. Furthermore, this model was calibrated only by limited test data that were available in 1970, which are not as reliable as more recent data.

Generalizing Bažant and Najjar's model [1], Sakata [4] obtained a similar expression which incorporates the effects of the water:cement ratio, in addition to age of concrete. However, he did not give general expressions for these parameters. Nor did he relate the observed phenomena to implied diffusion mechanisms, although this is essential in order to understand the time-dependent deformations of concrete.

The purpose of this article is to improve the model of Bažant and Najjar [1]. First the proper form of the diffusion equation will be formulated and its two coefficients, moisture capacity and diffusivity, will be described separately. The moisture capacity is defined as the derivative of the moisture content with respect to the relative humidity in a pore. Thus, the relationship between the moisture content and the relative humidity in a pore at constant temperature, called the adsorption isotherm, needs to be established, and then the moisture capacity follows. The first part of this study will deal with the adsorption isotherm and the second part [5] with the moisture capacity and diffusivity. A semiempirical expression for the adsorption isotherm will be developed by parametric analysis of the available adsorption test data. The effect of temperature will be included automatically, and the effects of water:cement ratio, age, and type of cement will also be taken into account.

Diffusion Equation

There are three different types of approaches to the diffusion problem: (1) a simple formulation based upon Fick's law, or Darcy's law [1], (2) computer sim-

ulation of flow through a random particle system [6–9], or (3) a formulation based directly on the basic physical laws, such as the kinetic theory of ideal gases and the conservation of mass and energy [10,11].

It is well established that, in cement paste, moisture moves from regions where it is plentiful to regions where it is scarce. This suggests that the moisture flux is proportional to the gradient of some variable which measures moisture content. However, the moisture flux may be expressed in two different ways. Either

$$J = -D_W \, \text{grad}(W_e) \tag{1}$$

with the mass balance equation

$$\frac{\partial W}{\partial t} = \frac{\partial (W_e + W_n)}{\partial t} = -\text{div}(J) = \text{div}(D_w \, \text{grad} \, W_e) \tag{2}$$

or

$$J = -D_h \, \text{grad} \, H \tag{3}$$

with

$$\frac{\partial W}{\partial t} = \frac{\partial W}{\partial H} \frac{\partial H}{\partial t} = -\text{div}(J) = \text{div}(D_h \, \text{grad} \, H). \tag{4}$$

H represents pore relative humidity, t is time, W is the total water content (for unit volume of material), W_e is the evaporable water content, and W_n is the nonevaporable, or chemically bound, water content. Equations 1 and 2 express the moisture flux in terms of the gradient of the water content. Equations 3 and 4 express the flux in terms of the gradient of the pore relative humidity (for isothermal conditions only). In eqs 1 to 4, D_w and D_h have different physical meanings: D_w represents moisture diffusivity, and D_h represents permeability, or humidity diffusivity [12].

In this study we use the formulation in terms of pore relative humidity, H, because the use of H appears to be more practical, for two reasons: (1) When the changes of evaporable water content due to hydration of cement are taken into account, one finds that, for usual water:cement ratios, the drop in H due to self-dessiccation caused by hydration (as in sealed specimens) is rather small, typically $H > 0.97$ [13]. In fact, it can be neglected even if hydration has not yet terminated. On the other hand, $\partial W_n/\partial t$(in eq 2) never has a negligible value unless hydration has ceased. (2) When generalization to variable temperature is considered, grad H can still be considered as a driving force of diffusion, but not grad W or grad W_e [2].

In eq 4, two coefficients must be determined: mois-

ture capacity, $\partial W/\partial H$, and diffusivity, D_h. Both coefficients depend on H, which causes the nonlinearity of eq 4. Independent test results will be used to evaluate the two coefficients. The moisture capacity, representing the derivative of the equilibrium adsorption isotherm, can be evaluated from test results. Therefore, the adsorption isotherm will be analyzed first, and then the diffusivity will be evaluated from drying tests [5].

Prediction Formula for Adsorption Isotherm

BET Model

The best known isotherm model is the famous Brunauer-Emmett-Teller (BET) model [14], derived from statistical thermodynamics of adsorption. But contrary to early assumptions, the range of validity to the BET equation for cement and concrete does not normally cover the relative pressures (humidity) from 0.05 to between 0.30 and 0.50; rather, it often covers only the range from 0.01 to 0.1 [15–17]. A host of attempts have been made to modify the BET equation in order to obtain better agreement with experimental isotherm data in the multilayer region. Some of the modified models are: the BDDT model [18]; the FHH model [19]; Hillerborg's formula [20]; and the BSB model [21], which is also called the three-parameter BET model, since it is a generalization of the BET model. The BSB model will be used in this study. It is applicable in the relative pressure range from 0.05 to 1.0, and reads:

$$W = \frac{C \, k \, V_m \, H}{(1 - kH)[1 + (C - 1) \, kH]} ,$$
$$C = \exp\left(\frac{E_1 - E_l}{RT}\right) \tag{5}$$

where $H = p/p_s$, p_s is the pressure at saturation; C and V_m are two constants used in the BET model (V_m = monolayer capacity); k is the third constant such that $k < 1$; E_1 is the total heat of adsorption per mole of vapor; E_l is the latent heat of condensation per mole; R is the gas constant; T is absolute temperature; and W is the quantity of vapor adsorbed at pressure p in grams of water per gram of cement paste.

The adsorption of water in hardened Portland cement paste is influenced by many parameters. In general, those that affect the adsorption isotherm include any parameter that contributes to the hydration process of Portland cement and hence to the constitution of the pore structure and the pore-size distribution. Some are as follows: the original water:cement ratio, w/c; type of cement, that is, the chemical composition

of the cement; curing time; temperature; curing method; carbonation (for structures with thin cross-sections); added ingredients such as accelerators, water reducers, retarders, superplasticizers, air entraining admixtures, or antifreezing admixtures; slag-cement [22]; sand-cement ratio, s/c; and gravel-cement ratio, g/c [23].

In this study, only the effects of the original water: cement ratio, w/c; age, t; temperature, T; and cement type are established in an empirical relationship with the amount of adsorption.

Monolayer Capacity

The monolayer capacity, V_m, is defined as the mass of adsorbate required to cover the adsorbent with a single molecular layer. Presently, there are several experimental methods in use to determine V_m [24,25]. The following empirical expression for V_m fits the observed test data:

$$V_m = V(t, w/c, c_t, T) = V_t(t)V_{wc}(w/c)V_{ct}(c_t)V_T(T) \quad (6)$$

where t is the age of specimen in days, and c_t indicates the type of cement. The functions in eq 6 may be characterized as follows.

1. $V_t(t)$—Figure 1 shows the effect of the curing time on the isotherms. The relationship between V_m and t is then obtained as shown in Figure 2. Figures 1 and 2 show V_m to increase as time increases. V_m, which depends upon the extent of hydration, approaches a
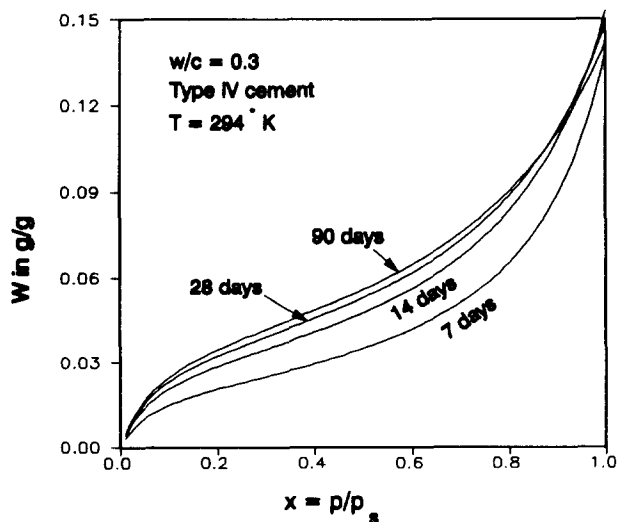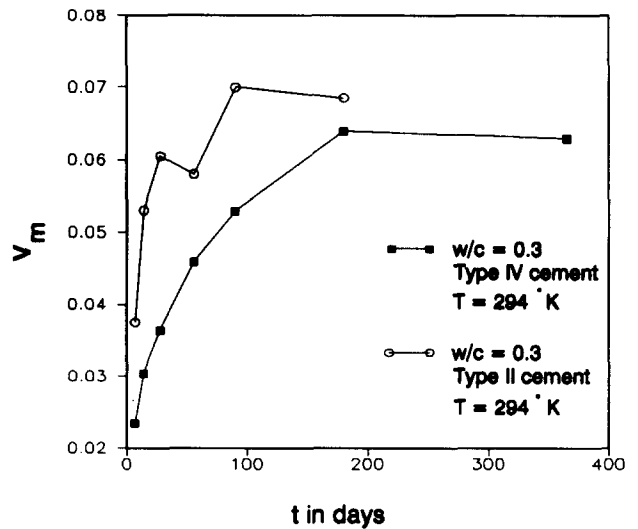

FIGURE 2. Dependence of monolayer capacity on concrete age t.

maximum at a curing time of approximately 6 months. Therefore, after 6 months of curing, the effect of age upon the adsorption isotherm of concrete may be excluded without any significant loss of accuracy. $V_t(t)$ is therefore assumed to be of the form a + b/t. Upon comparison with test data, $V_t(t)$ behaves according to the following empirical equation

$$V_t(t) = 0.068 - \frac{0.22}{t} \quad (7)$$

which is valid for $t \geq 5$ days. However, upon a check of test data gathered when $t < 5$ days [26,27], the V_m values corresponding to the range $0.25 \leq t \leq 4$ (in days) are almost equal to the value corresponding to $t = 5$ days. This indicates that after a certain surface area gets established in cement gel after the initial set, this area remains almost constant during five subsequent days, regardless of the curing period. Hence, for $t \leq 5$ days, V_t can be treated as constant; $V_t = 0.024$.

2. V_{ct}—The results of some of the adsorption tests are shown for various cements in Figure 3. For these data, Powers and Brownyard [28] did not classify the cement types for the specimens, but only the compound compositions. Upon comparison with the compositions of some commercial U.S. cements [29], the cements were classified into approximately four types.

In spite of extensive studies [22,28], the mechanism by which different compound compositions affect the shape of the adsorption isotherm is not clear. Therefore, we can only give empirical values obtained by fitting the data for different types of cements, in order to describe the effects of compound composition on the adsorption curves:
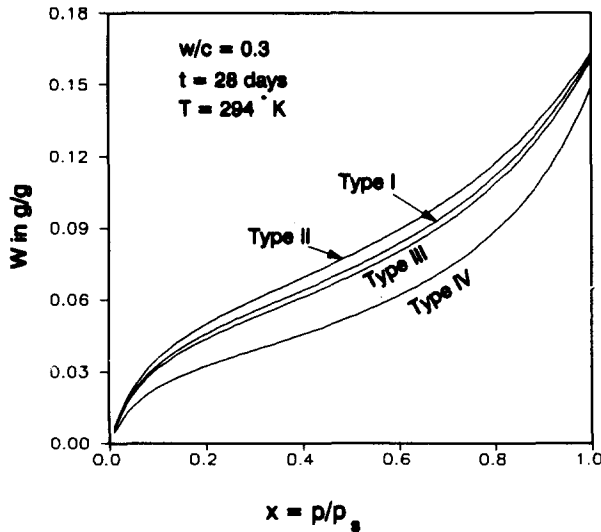

FIGURE 1. Effect of age t_0 at the start of drying on the adsorption isotherms.

FIGURE 3. Effect of the type of cement on the adsorption isotherms.

type 1: $V_{ct} = 0.9$; type 2: $V_{ct} = 1$; type 3: V_{ct} = 0.85; type 4: $V_{ct} = 0.6$. (8)

3. V_{wc}—Figure 4 shows that V_m is linearly related to the water:cement ratio, w/c, within the range 0.3 to 0.6. This relationship means that a low w/c corresponds to a low porosity and a low surface area. Therefore, V_m and w/c are assumed to be linked by a linear relation obtained from the test data:

$$V_{wc} = 0.85 + 0.45 \frac{w}{c}. \tag{9}$$

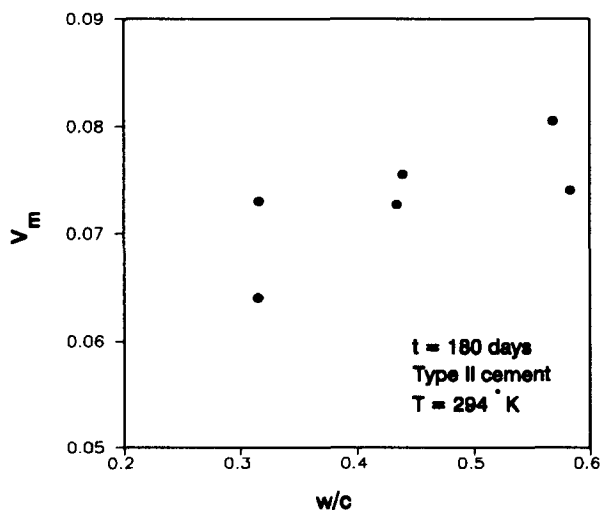However, for a low w/c such as 0.15, or a high w/c

FIGURE 4. Dependence of monolayer capacity on the water: cement ratio.

such as 0.75, no indication exists that this linear relation remains true. In low porosity pastes, it is in fact impossible for V_m to decrease with a very low w/c, and a limiting value may exist. Therefore, as an approximation, if the w/c falls below 0.3, V_{wc} should be taken as the value corresponding to $w/c = 0.3$, and if the w/c is above 0.6, V_{wc} should be taken as the value corresponding to $w/c = 0.6$.

Parameter C

Following the substitution, $C_0 = (E_1 - E_l)/R$, C in eq 5 becomes

$$C = \exp\left(\frac{C_0}{T}\right), \quad C_0 = T \ln(C) \tag{10}$$

where $E_1 - E_l$ is the net heat of adsorption, determined from heat of immersion experiments. As shown in Table 1, C varies from approximately 10 to 50. If V_m is held constant, the influence of temperature on the shapes of adsorption curves can be predicted from the present model, and one finds that near room temperature the adsorption curve changes with temperature only slightly. This means that the isotherms can be considered insensitive to changes in C within a rather wide range of values. Thus, it seems reasonable to forgo further analysis of C and simply assume that C_0 is constant. By eq 10, the expected value of C_0 can be obtained from test data; $C_0 = 855$ (coefficient of variation = 0.098). However, for high temperatures these simplifications are not possible and further phenomena need to be taken into consideration [2].

Parameter k

Parameter k of the BSB model results from the assumption that the number of adsorbed layers is finite, possibly even a small number [21]. To determine k, first the expression for the number of adsorbed layers at the saturation state, n, must be found, and n is then converted into parameter k, similar to the expression for V_m:

$$n = N(t,w/c, c_t, T) = N_t(t) \, N_{wc}(w/c) \, N_{ct}(c_t) \, N_T(T). \tag{11}$$

The influences of t and w/c on the parameter n are shown in Figures 5 and 6, respectively. The empirical equations for N_t and N_{wc} obtained by data fitting and the specific values of N_{ct} for different types of cements are as follows:

$$N_t(t) = 2.5 + \frac{15}{t} \tag{12}$$

TABLE 1. Test information and optimized parameters

V_m	C	k	n	w/c	t	T	Type
0.0234	15.14	0.8661	7.39	0.309	7.0	294.11	4
0.0302	17.94	0.8282	5.75	0.309	14.0	294.11	4
0.0364	27.16	0.8008	4.79	0.309	28.0	294.11	4
0.0462	25.37	0.7563	4.05	0.309	56.0	294.11	4
0.0525	21.99	0.7021	3.29	0.309	90.0	294.11	4
0.0644	15.31	0.6253	2.570	0.309	180.0	294.11	4
0.0619	23.19	0.6299	2.640	0.309	365.0	294.11	4
0.0371	23.84	0.7989	4.92	0.316	7.0	294.11	2
0.0529	14.32	0.6946	3.18	0.316	14.0	294.11	2
0.0609	10.42	0.6655	2.85	0.316	28.0	294.11	2
0.0580	33.86	0.6685	2.97	0.316	56.0	294.11	2
0.0696	15.84	0.5947	2.37	0.316	90.0	294.11	2
0.0680	13.91	0.6012	2.930	0.316	180.0	294.11	2
0.0512	18.77	0.7467	3.88	0.334	28.0	294.11	3
0.0368	22.61	0.8206	5.52	0.318	28.0	294.11	2
0.0319	19.30	0.8189	5.46	0.324	28.0	294.11	4
0.0465	19.70	0.7808	4.5	0.334	28.0	294.11	1
0.0562	15.96	0.6984	3.23	0.328	28.0	294.11	1
0.0558	20.62	0.7244	3.56	0.334	90.0	294.11	3
0.0530	16.90	0.7227	3.53	0.318	90.0	294.11	2
0.0447	22.24	0.7631	4.16	0.324	90.0	294.11	4
0.0556	19.53	0.7422	3.81	0.334	90.0	294.11	1
0.0669	12.43	0.6343	2.61	0.328	90.0	294.11	1
0.0609	10.42	0.6655	2.85	0.316	28.0	294.11	2
0.0657	9.637	0.7122	3.330	0.433	28.0	294.11	2
0.0632	11.61	0.7805	4.450	0.57	28.0	294.11	2
0.0494	34.60	0.7511	3.980	0.316	28.0	294.11	2
0.0492	34.19	0.7975	4.900	0.432	28.0	294.11	2
0.0481	45.45	0.8363	6.080	0.582	28.0	294.11	2
0.0680	13.91	0.6012	2.390	0.316	180.0	294.11	2
0.0701	13.51	0.7103	3.350	0.433	180.0	294.11	2
0.0751	17.05	0.7553	4.01	0.57	180.0	294.11	2
0.0590	22.54	0.6531	2.820	0.316	180.0	294.11	2
0.0678	15.11	0.7158	3.430	0.432	180.0	294.11	2
0.0690	13.77	0.7670	4.200	0.582	180.0	294.11	2
0.0613	9.753	0.6920	3.100	0.400	730.0	298.00	1
0.0642	18.60	0.7230	3.540	0.450	2555.0	298.00	1
0.0437	47.68	0.8820	8.450	0.700	730.0	298.00	1
0.0149	33.30	0.8740	7.940	0.200	1.000	298.00	2
0.0235	49.98	0.7380	3.790	0.200	3.000	298.00	2
0.0106	7.920	0.9230	12.99	0.200	0.250	308.00	1
0.0209	66.26	0.8070	5.160	0.200	1.000	308.00	1
0.0208	79.87	0.8240	5.680	0.200	3.000	308.00	1
0.0334	17.41	0.7380	3.740	0.200	7.000	308.00	1
0.0393	29.88	0.7190	3.510	0.200	28.00	308.00	1
0.0370	57.76	0.7270	3.640	0.200	90.00	308.00	1

and

$$N_{wc}(w/c) = 0.33 + 2.2\,\frac{w}{c} \tag{13}$$

provided that $t > 5$ days; otherwise, $N_t(t) = 5.5$. Furthermore,

type 1: $N_{ct} = 1.1$; type 2: $N_{ct} = 1$; type 3: $N_{ct} = 1.15$; type 4: $N_{ct} = 1.5$. $\tag{14}$

Equation 12 shows that, at saturation state, the average radii of the pores accessible to water decrease with progressing hydration. This has been experimentally confirmed by other investigators [26]. Equation 12 also gives some idea about the pore size at saturation state.

The expression for k is easily obtained from the expressions for n and C. From eq 5,

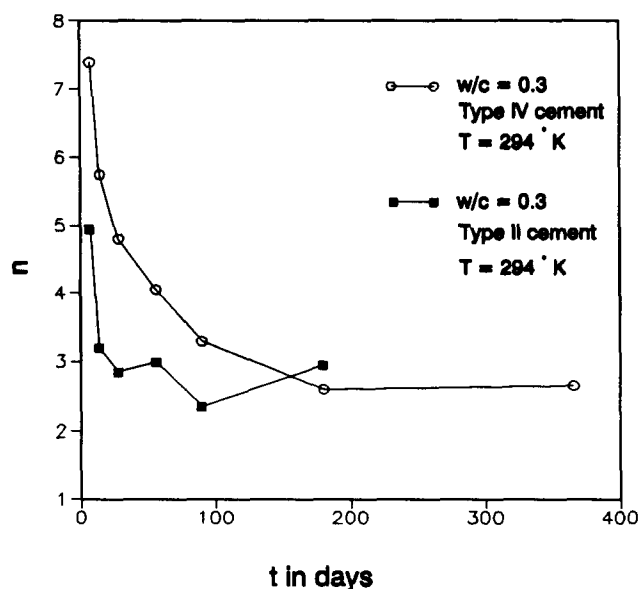$$n = \frac{W}{V_m} = \frac{C\,k\,H}{(1 - kH)[1 + (C - 1)kH]} \tag{15}$$

FIGURE 5. Dependence of parameter n on concrete age t.

Therefore, $H = 1.0$:

$$n = \frac{W}{V_m} = \frac{C\,k}{(1 - k)[1 + (C - 1)k]} \, . \qquad (16)$$

Then, from eq 16, an expression for k can be determined:

$$k = \frac{\left[2 - C\left(1 - \frac{1}{n}\right) \pm C\left(1 - \frac{1}{n}\right)\right]}{2(1 - C)} \, . \qquad (17)$$

FIGURE 6. Dependence of parameter n on the water:cement ratio.

If the positive sign in eq 17 is used, $k = 1/(1 - C)$. Upon comparison of the shapes of the experimental isotherms in Figures 1 and 3 with BDDT classifications [17,18], the isotherm curves for cement paste correspond to the type 2 isotherm. Hence, the values of C will be grater than 2.0 [15]. This is true for the test data in Table 1, which range form 10 to 50. Therefore, if the positive sign in eq 20 were used, k would be negative. However, the BSB model requires that k be within the range $0 < k < 1$ [21]. For this reason, the negative sign must be used in eq 20. The expression for k then becomes

$$k = \frac{\left(1 - \frac{1}{n}\right)C - 1}{(C - 1)} \qquad (18)$$

The condition $0 < k < 1$ is equivalent to the condition $0 < 1 - (1/n) < 1$; therefore, $n > 1$. At saturation state, the number of molecular layers covering a pore surface will always be greater than 1.

Influence of Temperature

Given one known isotherm, other unknown isotherms can be determined if the relationship of C, V_m, and k (or n) to temperature is studied. C is exponentially dependent on temperature. In eq 10, c_0 is related to the heat of adsorption. Although C_0 has been assumed to be constant, the reality is more complex. Actually, the values of C display no definite trend [17], nor do those of C_0, as seen in Table 1. Perhaps C_0 can be assumed to change only slightly with temperature [14], but this needs to be examined more carefully through further research. For the first approximation, C_0 may perhaps be taken as independent of temperature.

The variations of V_m with changes in temperature are due only to the thermal expansion or contraction of the adsorbed layer. The volumetric changes of the adsorbate, water, are very small at room temperature. Therefore, V_T may be taken as 1 in eq 6. For the same reason, n varies only slightly as well. In fact, empirical evidence shows that for moderate changes in temperature, the variation of n is negligible [15]. Therefore, in eq 11, N_T may also be taken as 1. k varies with temperature according to eq 18, since C is temperature dependent. For temperatures much higher than room temperature, and especially above 100°C, further phenomena come into play and a more complex model, based on the thermodynamic properties of water, is required (see ref 2).
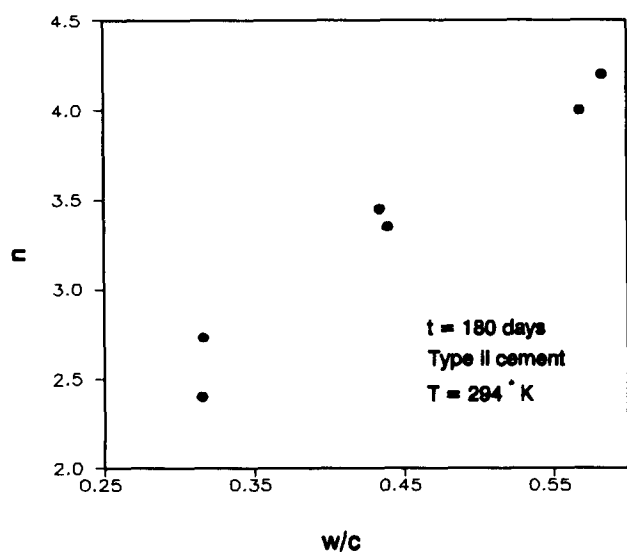
Proposed Model and Its Comparison with Test Data

The model and the final formulas for V_m, C, and k are as follows:

$$W = \frac{V_m\, C\, k\, H}{(1 - kH)[1 + (C - 1)kH]} \tag{19}$$

and

$$V_m = \left(0.068 - \frac{0.22}{t}\right)\left(0.85 + 0.45\,\frac{w}{c}\right) V_{ct}, \tag{20}$$

$$t > 5 \text{ days}, \ 0.3 < w/c < 0.7$$

but for $t \leq 5$ days, set t = 5 days; for $w/c \leq 0.3$, set w/c = 0.3; for $w/c \geq 0.7$, set w/c = 0.7; V_{ct} is given by eq 8; t is age of specimen in days; and

$$C = \exp\left(\frac{C_0}{T}\right), \ C_0 = 855 \tag{21}$$

TABLE 2. Optimized parameters and statistics

V_m	C	k	n	S_{s_m}	S_c	S_k	S_n
.0217	18.3032	.8496	7.0325	.9275	1.2089	.9809	.9516
.0310	18.3032	.8045	5.4096	1.0274	1.0202	.9713	.9408
.0357	18.3032	.7700	4.5982	.9805	.6739	.9615	.9600
.0380	18.3032	.7477	4.1925	.8230	.7215	.9886	1.0352
.0389	18.3032	.7381	4.0392	.7410	.8323	1.0513	1.2277
.0396	18.3032	.7297	3.9130	.6153	1.1955	1.1669	1.5226
.0400	18.3032	.7252	3.8490	.6461	.7893	1.1513	1.4580
.0363	18.3032	.7778	4.7599	.9781	.7678	.9735	.9675
.0519	18.3032	.7111	3.6614	.9807	1.2782	1.0238	1.1514
.0597	18.3032	.6601	3.1122	.9799	1.7565	.9919	1.0920
.0636	18.3032	.6272	2.8376	1.0961	.5406	.9383	.9554
.0650	18.3032	.6131	2.7339	.9345	1.1555	1.0309	1.1535
.0663	18.3032	.6006	2.6484	.9744	1.3158	.9990	.9039
.0511	18.3032	.7154	3.7173	.9988	.9751	.9581	.9581
.0597	18.3032	.6616	3.1256	1.6230	.8095	.8062	.5662
.0359	18.3032	.7772	4.7485	1.1265	.9484	.9491	.8697
.0541	18.3032	.7025	3.5557	1.1644	.9291	.8997	.7901
.0540	18.3032	.6988	3.5116	.9608	1.1468	1.0005	1.0872
.0557	18.3032	.6761	3.2654	.9989	.8876	.9333	.9172
.0651	18.3032	.6147	2.7456	1.2284	1.0830	.8506	.7778
.0392	18.3032	.7464	4.1712	.8762	.8230	.9781	1.0027
.0590	18.3032	.6613	3.1234	1.0615	.9372	.8910	.8198
.0589	18.3032	.6571	3.0847	.8798	1.4725	1.0359	1.1819
.0597	18.3032	.6601	3.1122	.9799	1.7565	.9919	1.0920
.0628	18.3032	.7283	3.8936	.9565	1.8993	1.0226	1.1693
.0665	18.3032	.7800	4.8086	1.0530	1.5765	.9994	1.0806
.0597	18.3032	.6601	3.1122	1.2080	.5290	.8789	.7820
.0628	18.3032	.7279	3.8869	1.2767	.5353	.9127	.7933
.0669	18.3032	.7836	4.8887	1.3903	.4027	.9370	.8041
.0663	18.3032	.6006	2.6484	.9744	1.3158	.9990	1.1081
.0698	18.3032	.6808	3.3134	.9953	1.3548	.9584	.9891
.0739	18.3032	.7415	4.0920	.9839	1.0735	.9817	1.0204
.0663	18.3032	.6006	2.6484	1.1230	.8120	.9196	.9392
.0697	18.3032	.6802	3.3077	1.0287	1.2113	.9503	.9643
.0743	18.3032	.7457	4.1602	1.0761	1.3292	.9723	.9905
.0628	17.6216	.6840	3.3548	1.0238	1.8068	.9884	1.0822
.0643	17.6216	.7086	3.6385	1.0020	.9474	.9801	1.0278
.0682	17.6216	.7683	4.5748	1.5616	.3696	.8710	.5414
.0226	17.6216	.7497	4.2350	1.5141	.5292	.8577	.5334
.0226	17.6216	.7497	4.2350	.9600	.3526	1.0158	1.1174
.0203	16.0543	.7711	4.6585	1.9155	2.0271	.8354	.3586
.0203	16.0543	.7711	4.6585	.9715	.2423	.9555	.9028
.0203	16.0543	.7711	4.6585	.9762	.2010	.9358	.8202
.0309	16.0543	.7288	3.9325	.9263	.9221	.9876	1.0515
.0509	16.0543	.5852	2.5713	1.2947	.5373	.8140	.7325
.0555	16.0543	.5279	2.2587	1.4989	.2779	.7261	.6205

TABLE 3. Statistics

	$M = 37$	$M = 46$
M_{v_m}	1.019	1.072
M_c	1.076	0.984
M_k	0.974	0.957
M_n	1.004	0.952
D_{v_m}	0.016	0.398
D_c	0.120	0.717
D_k	0.007	0.241
D_n	0.024	0.348

$M = 37$: The test data of the last nine rows in Table 1 ($w/c < 0.3$, and $w/c > 0.6$) are not included.
$M = 46$: All of the test data in Table 1 are included.

$$k = \frac{\left(1 - \frac{1}{n}\right) C - 1}{C - 1} \tag{22}$$

and

$$n = \left(2.5 + \frac{15}{t_e}\right)\left(0.33 + 2.2\frac{w}{c}\right) N_{ct},$$
$$t > 5 \text{ days}, \ 0.3 < w/c < 0.7 \tag{23}$$

but for $t \leq 5$ days, set $t = 5$ days; for $w/c \leq 0.3$, set $w/c = 0.3$; for $w/c \geq 0.7$, set $w/c = 0.7$; N_{ct} is given by eq 14.
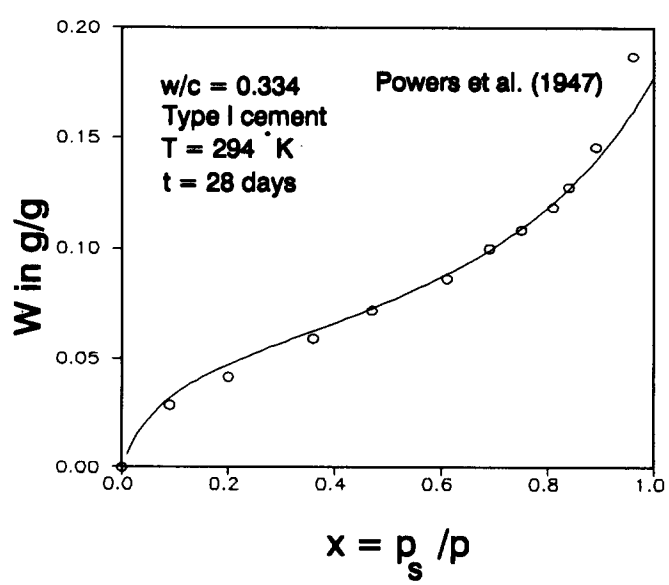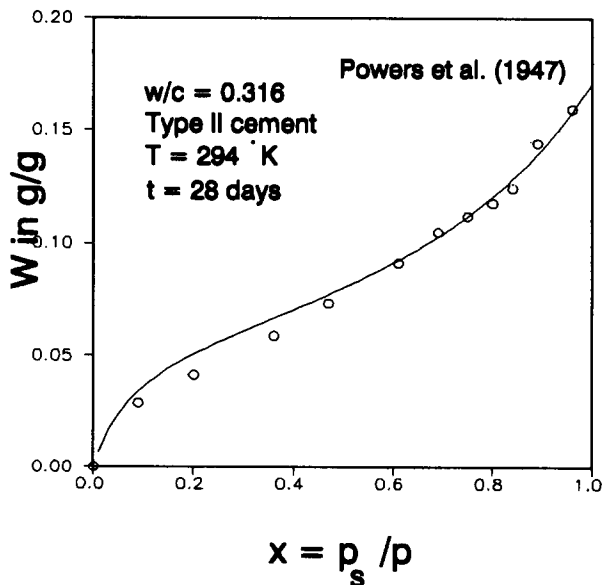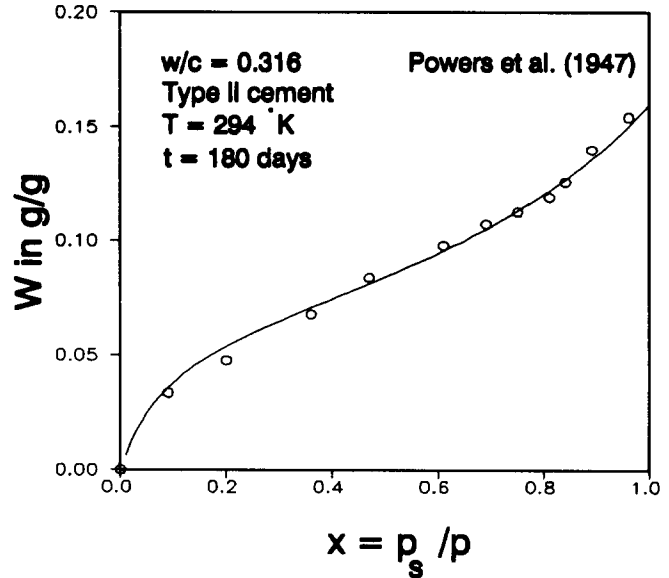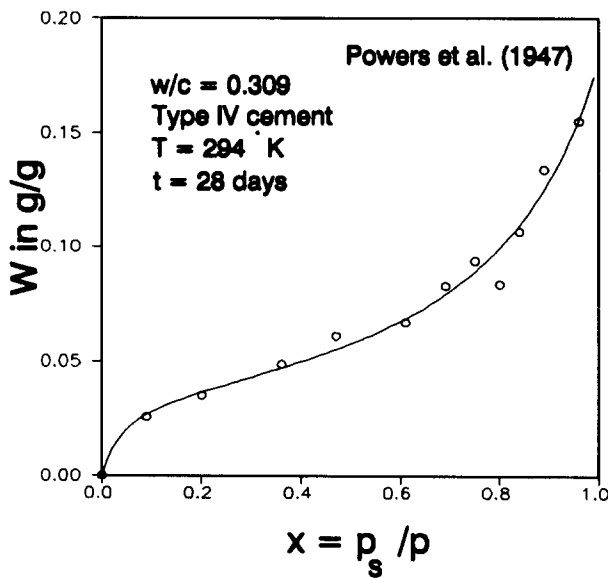
FIGURE 7. Comparison of predicted curves with isotherms measured for various concretes.
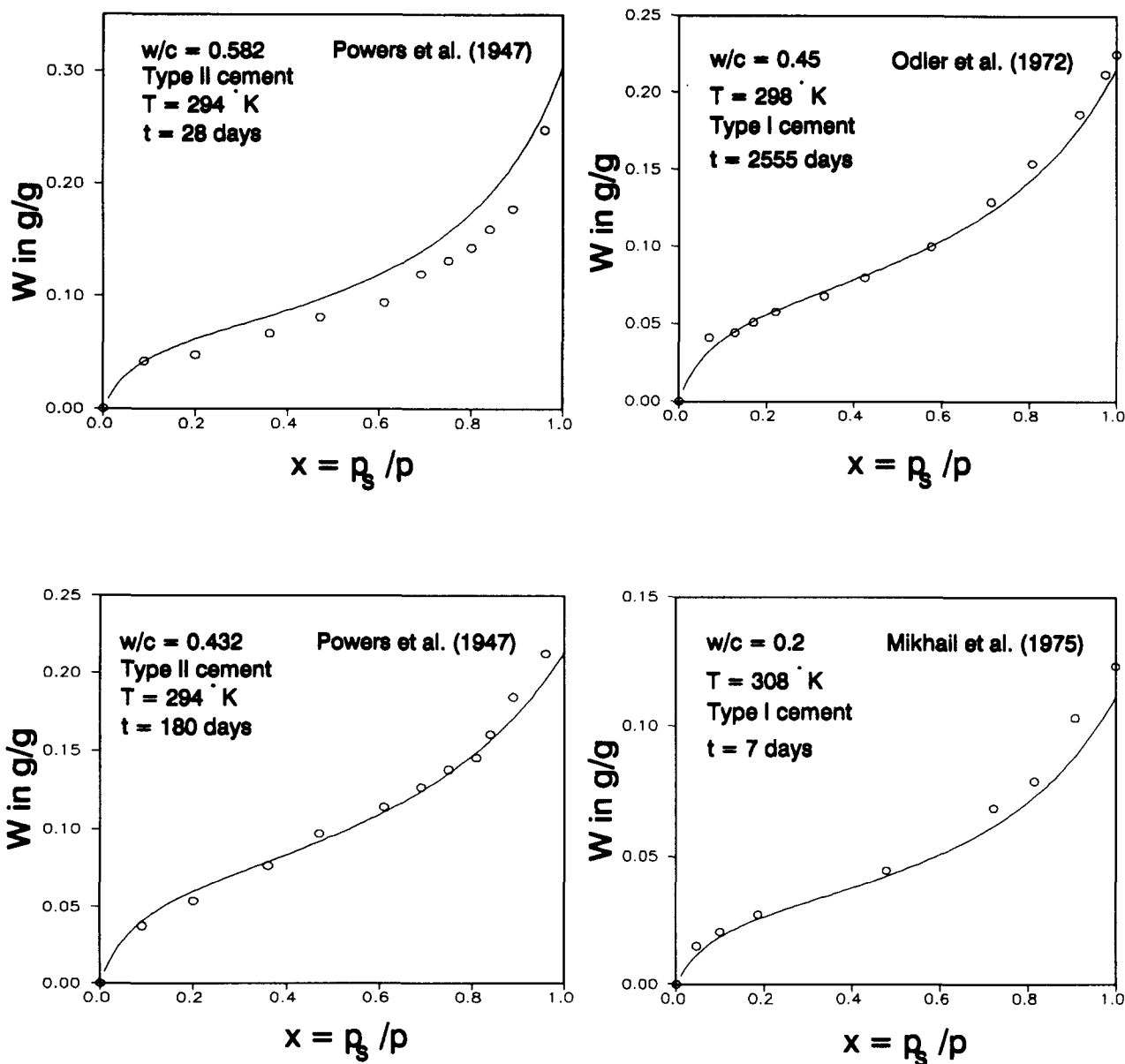
FIGURE 8. Further comparison of predicted curves with isotherms measured for various concretes.

Table 2 shows the calculated values of V_m, C, n, and k and the ratios of the calculated values to the test data S_{v_m}, S_c, S_n, and S_k, respectively, measured by Powers and Brownyard [28], Hagymassy et al. [27], and Mikhail and Abo-El-Enein [26]. Table 3 shows the expected values M_{vm}, M_c, M_n, and M_k of these ratios and the coefficients of variation D_{v_m}, D_c, D_n, and D_k. It is evident that the calculated results agree with the test data quite well (see the second column of Table 3, $M = 37$). Therefore, the present empirical equation can be used to estimate the parameters V_m, C, and n. Based on these parameters, approximate information about the pore structure, such as the surface area and the pore volume, can be obtained [30]. For the cases of

$w/c > 0.6$ and $w/c < 0.3$, the present formula is valid also, but the deviation from the real values increases (see the third column of Table 3, $M = 46$).

Figures 7 and 8 show comparisons of the calculated curves of the present empirical formulas with the measured curves. It is obvious that for different curing times, different w/c, and various cement types, these curves agree closely. This confirms that the chosen governing parameters, t, w/c, cement type and T, represent the major factors affecting the adsorption isotherms. Most importantly, this also confirms that the present semiempirical equation can represent the adsorption isotherm over the complete pressure range ($p/p_s = 0$ to 1).

Conclusions

1. The drying process of concrete can be described by the diffusion equation governing the pore relative humidity. The moisture capacity and diffusivity in the diffusion equation should be treated as two separate coefficients to be evaluated by independent test results. Both the moisture capacity and diffusivity depend on the pore structure of concrete, and the pore structure depends on the basic material parameters, such as the water:cement ratio, curing time, temperature, and type of cement.
2. The BSB model is chosen as a prediction model for the adsorption isotherm. Some empirical formulas are established for determining the three parameters of this model based on the available adsorption test data. The calculated results show that present empirical formulas predict the parameters quite accurately and therefore predict the adsorption isotherms for various Portland cement pastes very well.
3. The parameters V_m and n of the adsorption isotherm, predicted by the present formulas, can be used to obtain approximate information about the surface area, pore volume, and pore-size distribution on the basis of a given w/c, curing time, cement type, and temperature. This is useful for cases where the adsorption test data are unavailable.
4. Among the numerous parameters influencing the adsorption isotherm of Portland cement paste, the major parameters are the curing time, water:cement ratio, cement type, and temperature. The results show that: (1) the temperature does not have much influence on the isotherm in the range of room temperatures; (2) after 6 months of curing, the parameters V_m and n, which represent the monolayer capacity and the number of adsorbed layers at saturation, are almost independent of the curing time; and (3) w/c has a linear relationship with V_m and n, and it seems that at $w/c = 0.6$, V_m and n reach their maximum values.

Acknowledgments

References

1. Bažant, Z.P.; Najjar, L.J. Matériaux et Constructions 1972, 5, 3–20.

2. Bažant, Z.P.; Thonguthai, W. J. Eng. Mech. Div., Proceedings, ASCE 1978, 104, 1059–1079.

3. Bažant, Z.P.; Wittmann, F.H., Eds. Mathematical Models for Creep and Shrinkage of Concrete; John Wiley & Sons: New York, 1982; pp 163–256.

4. Sakata, K. Cement Concrete Res. 1983, 13, 216–224.

5. Xi, Y.; Bažant, Z.P.; Molina, L.; Jennings, H.M. J. Adv. Cement Based Mater. 1994, 1, 258–266.

6. Kamp, C.L.; Roelfstra, P.E.; Wittmann, F.H. Proc. Int. Conf. on Struc. Mech. In Reactor Tech. (SMiRT), Lausanne, 1987, H, 157–166.

7. Garboczi, E.J. Cement Concrete Res. 1990, 20, 591–601.

8. Garboczi, E.J.; Bentz, D.P. In Scientific Basis for Nuclear Waste Management XIII, MRS Symposium Series Proc.; Oversby, V.M.; Brown, P.M., Eds.; Materials Research Society: Pittsburgh, PA, 1990.

9. Schwartz, L.M.; Banavar, J.R. Phys. Rev. B 1989, 39, 11965–11970.

10. Huang, C.L.D.; Siang, H.H.; Best, C.H. Int. J. Heat Mass Transfer 1979, 22, 257–266.

11. Chou, W.T-H.; Whitaker, S. Proc. of the Third International Drying Symposium 1982, 1, 135–148.

12. Jonasson, J.-E. Proc. Int. Conf. on Struc. Mech. in Reactor Tech. (SMiRT), Brussels, 1985, H5/11, 235–242.

13. Copeland, L.E.; Bragg, R.H. Proc. Am. Soc. for Testing Materials 1955, 204 (PCA Bulletin 52).

14. Brunauer, S.; Emmett, P.H.; Teller, E. J. Am. Chem. Soc. 1938, 60, 309–319.

15. Gregg, S.J.; Sing, K.W.S. Adsorption, Surface Area and Porosity; Academic Press, Inc.: London, 1982.

16. Mikhail, R.S. Microstructure and Thermal Analysis of Solid Surfaces, John Wiley & Sons: New York, 1983.

17. Brunauer, S. The Adsorption of Gases and Vapors, Princeton University Press: Princeton, NJ, 1943.

18. Brunauer, S.; Deming, L.S.; Deming, W.E.; Teller, E. J. Am. Chem. Soc. 1940, 62, 1723–1732.

19. Halsey, G. J. Chem. Phys. 1948, 16, 931–937.

20. Hillerborg, A. Cement Concrete Res. 1985, 15, 809–816.

21. Brunauer, S.; Skalny, J.; Bodor, E.E. J. Colloid Interface Sci. 1969, 30, 546–552.

22. Mikhail, R.S.; Abo-El-Enein, S.A.; Gabr, N.A. J. Appl. Chem. Biotechnol. 1975, 25, 835–847.

23. Gleysteen, L.F.; Kalousek, G.L. J. Am. Conc. Inst. 1955, 26, 437–446.

24. Young, D.M.; Crowell, A.D. Physical Adsorption of Gases; Butterworths: Washington, 1962.

25. Adamson, A.W. Physical Chemistry of Surfaces, 4th ed; John Wiley & Sons: New York, 1982.

26. Mikhail, R.S.; Abo-El-Enein, S.A. Cement Concrete Res. 1972, 2, 401–414.

27. Hagymassy, J., Jr.; Odler, I.; Yudenfreund, M.; Skalny, J.; Brunauer, S. J. Colloid Interface Sci. 1972, 38, 20–34; 265–276.

28. Powers, T.C.; Brownyard, T.L. Proc. Am. Conc. Inst. 1946–1947, 43, 101, 149, 469, 549, 845, 933.

29. Ramachandran, V.S. Concrete Admixtures Handbook: Properties, Science, and Technology; Noyes Publications, 1984.

30. Brunauer, S.; Mikhail, R.S.; Bodor, E.E. J. Colloid Interface Sci. 1967, 24, 451–463.

Moisture Diffusion in Cementitious Materials

Moisture Capacity and Diffusivity

Yunping Xi, Zdeněk P. Bažant, Larissa Molina, and Hamlin M. Jennings
Department of Civil Engineering, Northwestern University, Evanston, Illinois

Based on a model by Bažant and Najjar, and using a new model for adsorption isotherms, moisture capacity and diffusivity of concrete are analyzed. The moisture capacity, obtained as a derivative of the adsorption isotherm, first drops as the humidity increases from zero, then levels off as a constant, and finally again increases when the humidity approaches saturation, regardless of the age, cement type, temperature, and water:cement ratio. The well-known diffusion mechanisms, including the ordinary diffusion, Knudsen diffusion, and surface diffusion, are analyzed and the diffusion in concrete is treated as a combination of these mechanisms. An improved formula for the dependence of diffusivity on pore humidity is proposed. The improved model for moisture diffusion is found to give satisfactory diffusion profiles and long-term drying predictions. The model is suited for incorporation into finite element programs for shrinkage and creep effects in concrete structures. ADVANCED CEMENT BASED MATERIALS 1994, 1, 258–266

KEY WORDS: Adsorption, Concrete, Hardened cement paste, Moisture diffusion, Moisture effects, Permeability, Porosity

Moisture diffusion is very important for the long-term performance of cementitious materials. The moisture diffusion can be described by diffusion equations and solved by various numerical methods, provided that the coefficients are known. However, even though the diffusion-related coefficients have long been studied in the research on transport behaviors of the materials, they still remain an unsolved problem, although many different models have been proposed [1–5].

The major difficulty in establishing reliable diffusion parameters is that diffusion of moisture inside cementitious materials is basically controlled by the microstructure of the material, and especially by the pore-size distribution. The microstructure is changing with age as well as with relative humidity in the pores. Therefore, all of the parameters, such as the water/cement ratio, type of cement, and curing time, which affect the formation of the microstructure of cementitious materials, have significant effects on diffusion

parameters. However, few models proposed in the literature have taken enough parameters. Most recently, Daian [2,3] proposed a model for mortar in which the pore-size distribution is analyzed and the relationship between the diffusivity and the diffusion mechanisms is explored. But this model was not calibrated with available test results and did not take into account all the relevant influencing parameters. In the context of freeze-thaw analysis, Bažant et al. [6] developed a model for the isotherms based on the filling of capillary meniscus and the pore-size distribution. This model, however, does not cover gel pores.

For the two reasons mentioned in the preceding article [7], the basic idea from Bažant and Najjar [1] is followed in this article. An expression for moisture diffusion is formulated in terms of the relative humidity. Some other models which use the moisture content as the basic variable have also been formulated [8–10]. However, they have some limitations [1,7]. In any case, a formulation of drying in terms of the relative humidity, rather than moisture content, is preferable.

Xi et al. [7] present a diffusion equation that has been formulated in terms of two separate parameters, the moisture capacity and the diffusivity, both of which control the diffusion process. This is a natural result of abandoning the approximation that assumes the slope of adsorption isotherm to be constant. Both of the parameters are considered to be functions of the relative humidity in the pores, which makes the problem nonlinear. Because the moisture capacity is the derivative of the adsorption isotherm, the adsorption isotherm must be studied first [7]. A semiempirical formula for the adsorption isotherm has been established based on the available test results for the water adsorption isotherm. The effects of water:cement ratio, temperature, type of cement, and curing time have been taken into account.

The main purposes of this article are, first, to analyze how moisture capacity is related to the parameters: water:cement ratio, curing time, temperature, and type of cement, and second, to assess qualitatively the diffusivities corresponding to various diffusion mech-
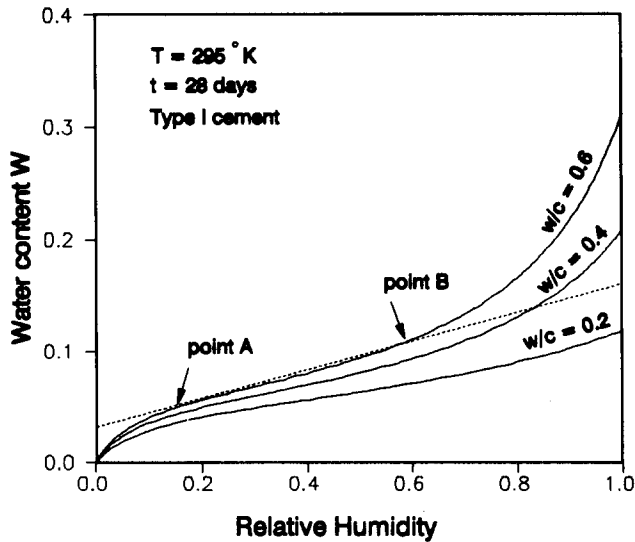
FIGURE 1. Effect of water-cement ratio on sorption isotherms.

anisms and the influences of the water:cement ratio. Finally, an empirical formula for diffusivity is proposed and calibrated by recent data on diffusion. The resulting general expression can be employed in practice.

Moisture Capacity

The diffusion equation for cementitious materials reads [7]:

$$\frac{\partial W}{\partial H} \frac{\partial H}{\partial t} = \text{div}(D_h \text{ grad } H) \tag{1}$$

where the moisture capacity, represented by $\partial W/\partial H$, can be obtained from the equilibrium adsorption isotherm (derivative of eq 19 in ref 7):

$$\frac{\partial W}{\partial H} = \frac{CkV_m + Wk[1 + (C - 1)kH] - Wk(1 - kH)(C - 1)}{(1 - kH)[1 + (C - 1)kH]} . \tag{2}$$

Figures 1 to 3 illustrate the influences of the water-cement ratio and age on the isotherms and moisture capacity curves. The effect of age is analogous to the effect of the degree of hydration, which was analyzed by Jonasson [4].

From Figures 2 and 3 it is evident that moisture capacity is not a constant. First it drops, then it becomes constant, and finally it increases. The physical meaning of such a variation in moisture capacity may be explained by comparing Figure 1 with Figure 2. The first turn point in Figure 2 corresponds to point A in

Figure 1. At this point, the adsorbent reaches its monolayer capacity, above which the moisture capacity does not decrease steeply with increasing H. The second turn point in Figure 2 corresponds to point B in Figure 1. This is the initial point of capillary condensation. For the usual practical range (from 50 to 100%), one can see that the moisture capacity increases.

Equation 1 can be rearranged as follows:

$$\frac{\partial H}{\partial t} = \frac{\partial H}{\partial W} \text{ div}(D_h \text{ grad } H). \tag{3}$$

The curves of $\partial H/\partial W$, which is the reciprocal of moisture capacity, are shown in Figure 4 for various values of w/c. Figure 5 shows the effects of different ages upon $\partial H/\partial W$. From Figures 4 and 5 one can also see clearly that $\partial H/\partial W$ is not a constant. This is one of the improvements over the previous model of Bažant and Najjar [1].

Note that the present adsorption isotherm was based upon test data for cement paste. To apply the adsorption isotherm to concrete, a few additional effects need to be considered, such as the aggregate content. However, few test data for concrete are found in the literature [11].

Another point requiring explanation is why we have limited our attention to the adsorption isotherms even though, strictly speaking, desorption isotherms should be used for drying processes, and adsorption isotherms for wetting processes. Actually, the exact values of the adsorption and desorption curves are not as important as the shapes of the curves if we study one-way drying or one-way wetting only. In fact, upon comparison of experimental results, it is apparent that
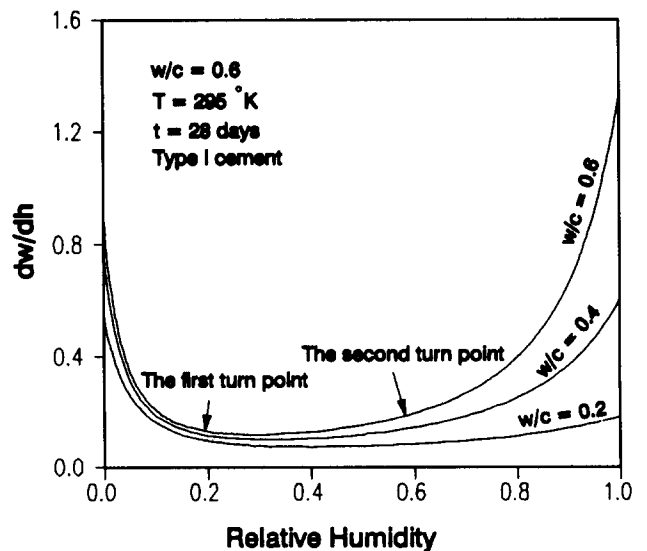

FIGURE 2. Effect of water:cement ratio on moisture capacity.
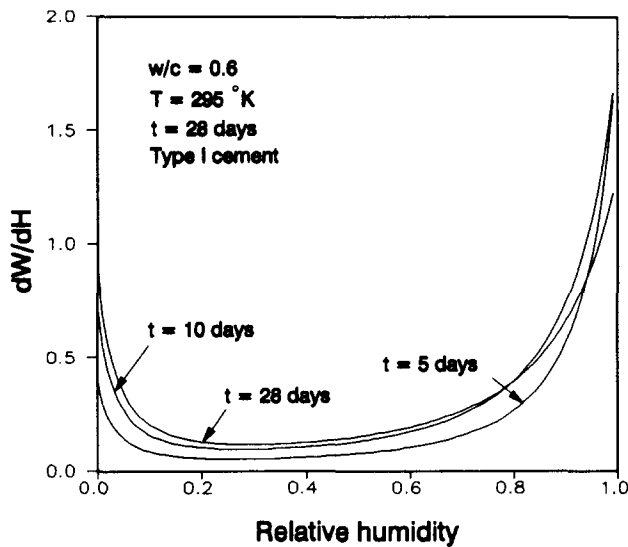
FIGURE 3. Effect of age on moisture capacity.

adsorption and desorption curves possess virtually the same shape [12,13]. This can be checked further by classification of the hysteresis loops. According to de Boer's classification [14], the cement paste displays a loop of type B. Another classification recommended in the International Union of Pure and Applied Chemistry (IUPAC) manual [14] shows that the cement paste displays a loop of type H3. Both classifications indicate that adsorption and desorption have nearly the same shape in the practical range of H. On the other hand, the BSB model (eq 19 in ref 7) is valid for both adsorption and desorption. Additionally, since systematic experimental results on adsorption are much more abundant in the literature than those for desorption, the use of the adsorption isotherm is most convenient.

In eq 3, $\partial H/\partial W$ can be computed by the adsorption isotherm for a given w/c, t_0, type of cement, and temperature [7]. Therefore, the only unknown coefficient that remains in eq 3 is the diffusivity.

Diffusivity and Diffusion Mechanisms

Diffusivity of concrete depends strongly on the diffusion mechanisms. Diffusion mechanisms are influenced by the pore structure of concrete. Three distinct transport mechanisms may operate singularly or simultaneously: molecular diffusion (ordinary diffusion), Knudsen diffusion, and surface diffusion. Thus, the total diffusivity is a complex property that often includes contributions from multiple mechanisms [15]. Although each individual mechanism is reasonably understood, it is not always easy to make an accurate prediction of the total diffusivity because it depends strongly on the details of the pore structure.

Figure 6a shows the molecular diffusion process inside the macropores (capillary pores) of concrete. At a low relative humidity level, the field force of the pore wall captures water molecules to form the first attached layer. Other water molecules continue to move ahead and, as the humidity increases, more layers of water molecules cover the pore walls. As a result, the free space available to vapor inside the macropore decreases. However, the force field of the wall thus weakens and, at the same time, the mean free path of water molecules decreases because the mean free path of water molecules, surrounded by the solid wall with water molecules attached to it, is smaller than the mean free path of water molecules surrounded only by solid walls. These trends affect the resistance to diffusion oppositely.

When the pore humidity is high enough, the adsorbed water will form a meniscus at a neck (a narrow connection between larger pores). At high humidity, menisci form on both ends of the neck, and the neck is completely filled. At this point, water molecules condense at one end of the neck, while at the other end they evaporate, as shown in Figure 6b. Since part of the transport is through gas, this condensation and evaporation process strongly accelerates the diffusion process.

The foregoing diffusion process will dominate whenever the mean free path of the water vapor (which is 800 Å at 25°C) is small relative to the diameter of the macropore, which is generally regarded to have a diameter of about 50 nm to 10 μm [16]. Pores of this size constitute only a small portion of the pores in concrete. Therefore, molecular diffusion or ordinary
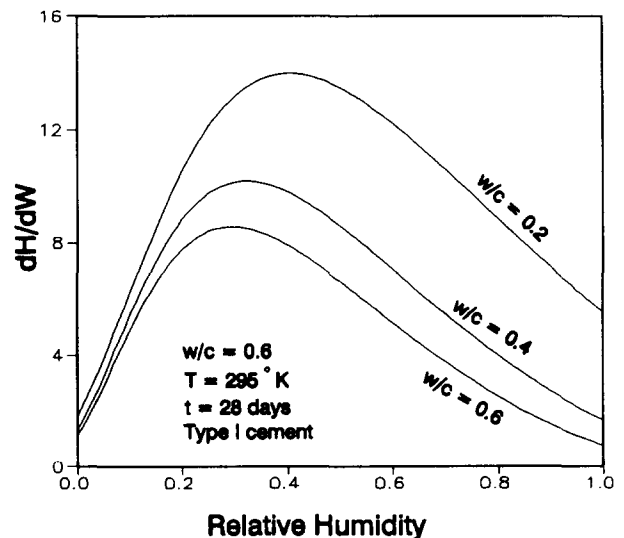

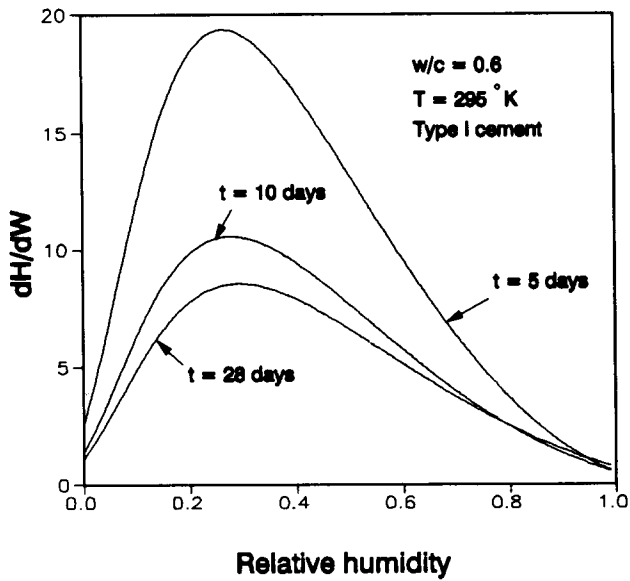**FIGURE 4.** Effect of water-cement ratio on reciprocal of moisture capacity.

FIGURE 5. Effect of age on reciprocal of moisture capacity.

diffusion occurs in concrete only occasionally. It is not a dominant mechanism.

Mesopores (25 to 500 Å) and micropores (<25 Å) comprise the largest portion of concrete pores. In these pores, the collisions between molecules as well as against pore walls provide the main diffusion resistance. In that case, the diffusion is called Knudsen diffusion. Similar phenomena occur at various humidity levels, but a difference exists between molecular diffusion and Knudsen diffusion. For Knudsen diffusion, the diffusion resistance is related to pore size. Some formulas for Knudsen diffusion in straight cylindrical pores have been deduced [2,17]. However, for cement matrix, which is an amorphous colloidal material with randomly oriented pores and variable pore radii, it is necessary to consider the pore connections
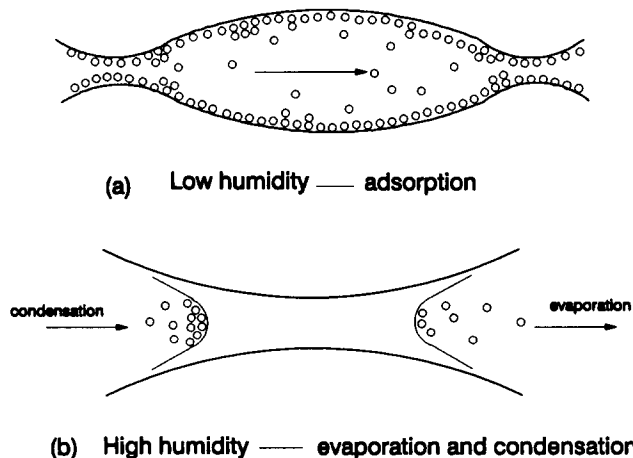
and tortuosity. For smaller pores, the resistance is larger and thus the diffusivity is smaller.

Figure 7 displays the surface diffusion process that occurs in certain mesopores and micropores, such as the pores of parallel walls. The water molecules never escape the force field of the pore surface. The transport involves a thermally activated process with jumps between the adsorption sites. Such a process, representing the surface diffusion, poses greater resistance to transport than Knudsen diffusion for pore sizes typical of concrete. Thus, the surface diffusion is insignificant unless most of the water is adsorbed water. Therefore, surface diffusion is significant in concrete only at very low humidity.

To sum up, water diffusion in concrete occurs by one or more of the three mechanisms described: (1) ordinary diffusion, (2) Knudsen diffusion, and (3) surface diffusion. When multiple mechanisms occur, their effects do not necessarily combine in a simple manner. Previous investigators obtained some models for each mechanism individually. Since they based their results upon diffusion in regular cylindrical pores, a tortuosity factor was introduced to correct for pore irregularity. The contributions of each mechanism were then combined [2,17,18]. However, as mentioned above, the pore structure changes when the water-cement ratio changes. Furthermore, the formation process of fine micropores depends strongly on time and humidity level. Therefore, it is difficult to derive a general expression for diffusivity. The model we will now present does not treat each mechanism individually, but tries to predict the general combined trend.

Upon comparison of all three diffusion mechanisms, it is clear that they share similarities. At low humidity, the pore volume decreases, the surface force field weakens, and the mean free path decreases. These behaviors may just offset each other such that the effective diffusivity for all the mechanisms becomes con-

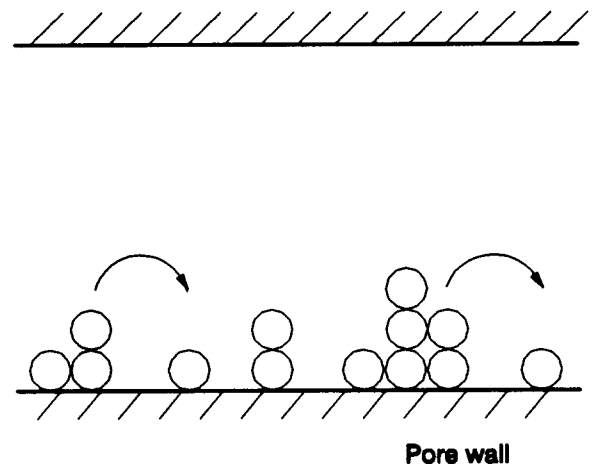FIGURE 6. Diffusion mechanisms at different humidity levels.

FIGURE 7. Mechanism of surface diffusion.

stant at low humidity (see Figure 8). At high humidity, capillary condensation occurs and hence the diffusion resistance lessens. Consequently, the effective diffusivity of the system may be assumed to follow the simple empirical curve shown in Figure 8d. The inevitable empirical aspect of this curve makes it unnecessary, and in fact unjustified, to distinguish among these mechanisms. The following simple empirical formula, which can capture the aforementioned trends, is proposed:

$$D_h = \alpha_h + \beta_h\left[1 - 2^{-10^{\gamma h(H-1)}}\right]. \tag{4}$$

Here, α_h, β_h, and γ_h are coefficients to be calibrated from test data (Figure 9 displays their meanings). α_h represents the lower bound on diffusivity approached at low humidity level. The value of $\beta_h/2$ is the diffusivity increment from low humidity level to saturation state; γ_h characterizes the humidity level at which the diffusivity begins to increase.

The coefficients α_h, β_h, and γ_h are strongly affected by w/c. The effect of curing time on these coefficients could be regarded as negligible. The curing time, of course, does affect the diffusion process, but this is taken into account by the moisture capacity.
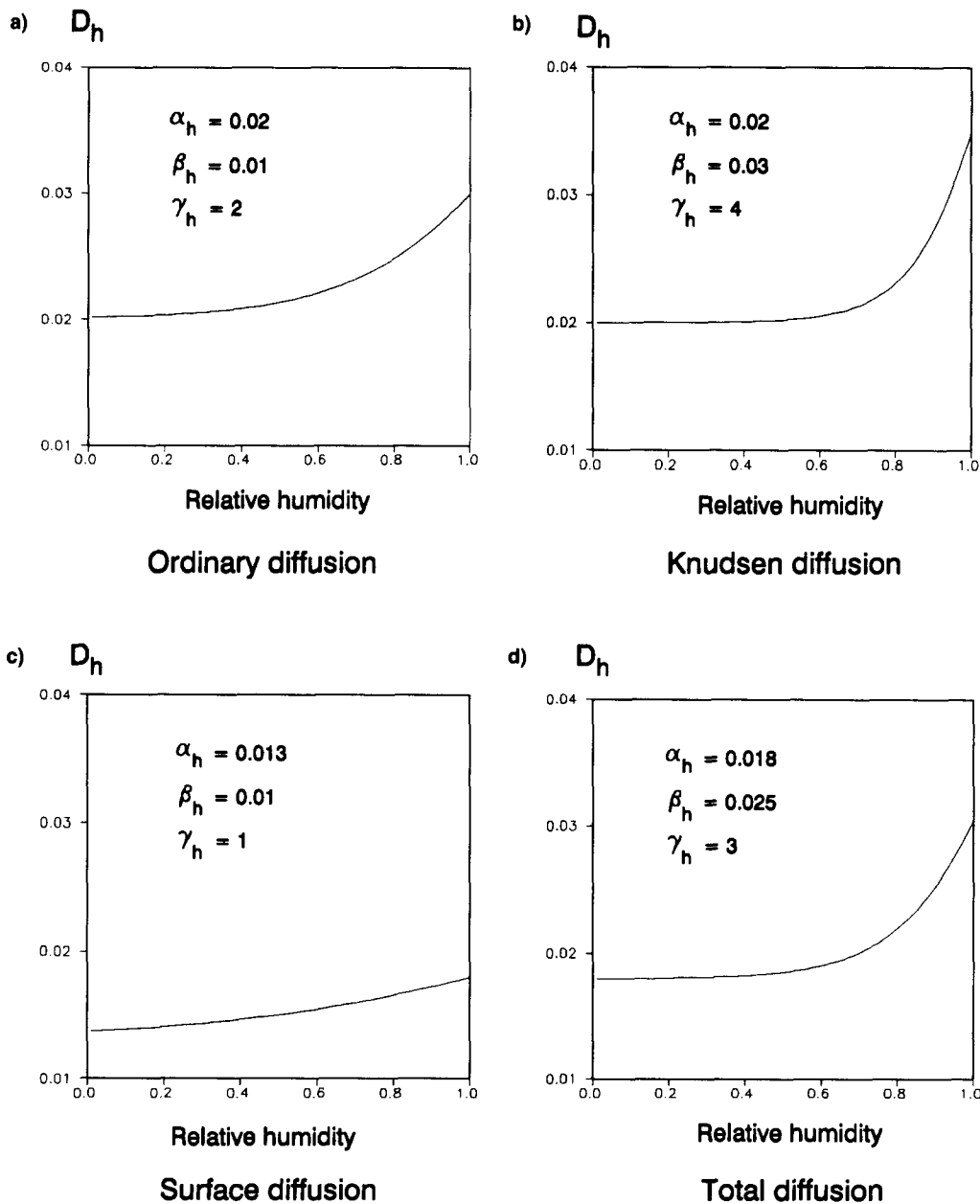

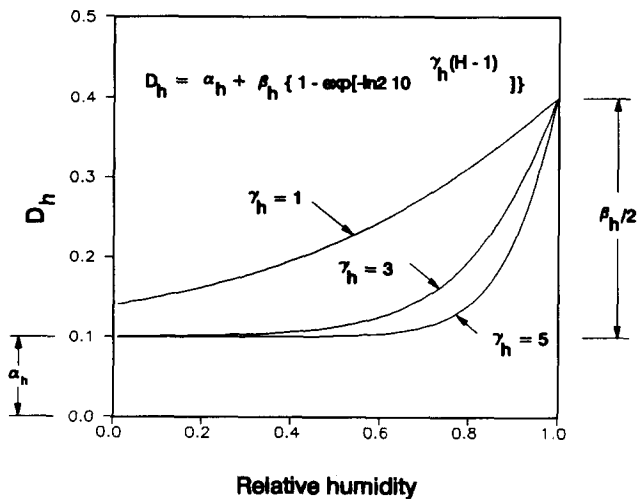FIGURE 8. Diffusivity dependence on humidity for various diffusion mechanisms and for their combined effect.

FIGURE 9. Diffusivity dependence on humidity for various values of parameter γ_h.
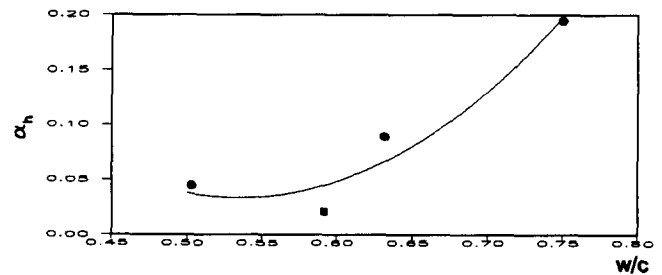

FIGURE 10. Dependence of α_h on water-cement ratio of concrete mix.

Calibration by Test Results

Two methods are used to identify D_h from test results. First, upon application of the Boltzmann transformation [19] to eq 3, the diffusivity in eq 3 can be expressed as follows: $D_h(H) = \int_H^1 u/(2dH/du)$, dH, where $u = y/\sqrt{t}$ is the Boltzmann variable, and y is the depth from the surface of drying. This method, however, is valid only when the diffusion equation is linear, that is, when the moisture capacity in eq 3 is constant. The second method consists of trial and error selections of various expressions for D_h, such as eq 4. For each selection, the nonlinear diffusion equation must be solved numerically to determine which selection best fits the experimental results. The optimum values of the coefficients in the formula can be found by an optimization algorithm that minimizes the sum of squared deviation from test data, which has been used in the present study.

The equation to be solved is the same as eq 3. Assuming that drying occurs only in one dimension, we have the diffusion equation with the boundary and initial conditions

Before calibrating eq 4 with test data, the possible relations between α_h, β_h, γ_h, and w/c must be analyzed. As described earlier, the porosity increases as w/c increases. This means that the volume fraction of macropores increases also. As a result, the diffusivity at low humidity levels increases with increasing w/c because water molecules migrate much faster in the macropores than in the micropores. Thus, α_h generally increases with increasing w/c. As for β_h, it first increases with increasing w/c, for the same reason as does α_h. After a certain point, however, β_h decreases with increasing w/c because the increase of diffusivity from a low humidity level to the saturation state will gradually weaken with increasing volume fraction of macropores. An increase in w/c leads to an increase in γ_h. From Figure 9, a larger γ_h corresponds to a higher humidity level at which the diffusivity initially begins to increase, and it also corresponds to a higher rate of diffusivity increase. This trend is reasonable because a higher w/c corresponds to a larger volume fraction of macropores, and because the humidity level, or the pressure level, necessary for capillary condensation is higher in a larger pore than in a smaller pore, according to capillary theory. Knowledge of the foregoing general trends is helpful to choose a correct function to be calibrated by drying test results (Figures 10–12).

$$\frac{\partial H}{\partial t} = \frac{\partial H}{\partial W} \frac{\partial}{\partial x}\left(D_h \frac{\partial H}{\partial x}\right) \qquad (5a)$$

for $t = 0$, $0 \leq x \leq 1$: $H = 1$
for $x = 1$, $t > 0$: $\quad H = 0$ $\qquad$ (5b)
for $x = 0$, $t > 0$: $\partial H/\partial x = 0$.

TABLE 1. Test information and optimized parameters

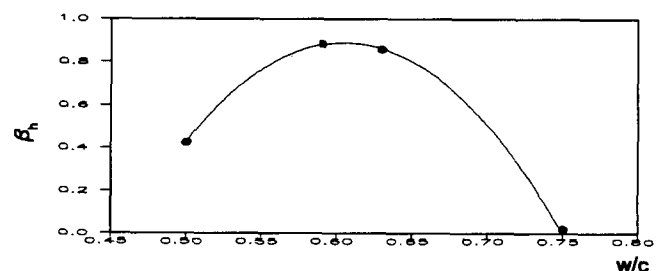| No.	w/c	t_o	l	α_h	β_h	γ_h
66-07-08	0.657	7	7.5	0.003	5.170	7.03
66-28-08	0.657	28	7.5	0.003	5.240	7.66
50-03-15	0.50	3	15.0	0.0423	0.432	3.54
59-01-10	0.59	1	10.0	0.020	0.875	8.97
63-03-15	0.63	3	15.0	0.088	0.864	8.58
75-03-15	0.75	3	15.0	0.195	0.002	20.60

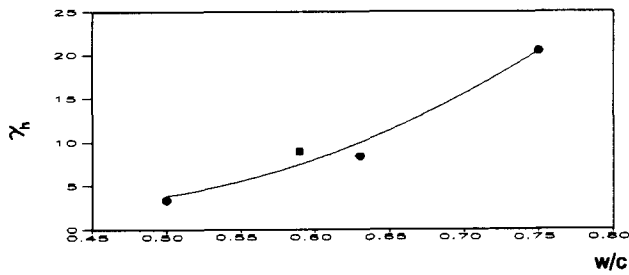**FIGURE 11.** Dependence of β_h on water:cement ratio.

FIGURE 12. Dependence of γ_h on water:cement ratio.

This diffusion problem is solved by the Crank-Nicolson finite difference algorithm [20] for both cylindrical and Cartesian coordinate systems. D_h (eq 4) is a function with unknown parameters α_h, β_h, and γ_h. Therefore, a nonlinear curve-fitting program is used and the program for the finite difference solution is combined with a nonlinear optimization subroutine in order to calibrate the three parameters with available test data.

An important point is the effect of age. The specimens for adsorption test were cured up to t_0 days, and then all the evaporable water held inside the specimen was evaporated by the vacuum method. After this process the pore structure is supposed to be the same as that at age t_0, since the hydration process ceases when the pore relative humidity drops below approximately $H = 0.8$ [21]. This means that time t in the equations of adsorption isotherm [7] corresponds roughly to the time when the hydration process terminates, and the termination of the process depends mainly on the pore relative humidity. For real drying specimens, the pore relative humidity in the outer layers drops after a short exposure to the environment, while the inner pores are still under conditions similar to the curing room. Thus, the age t is actually an equivalent age t_e, not the real age, and it is significantly different at different locations.

For the numerical solution, an equivalent time increment Δt_e may be assumed to be a function of the relative humidity in the pores as follows [1]:

$$\Delta t_e = \Delta t \big[1 + (7.5 - 7.5H)^4\big]^{-1} \qquad (6)$$

where Δt is the real age increment when the specimen is cured in a fog room. Equation 6 satisfies two asymptotic trends. When H is near saturation, $\Delta t_e = \Delta t$, and when H approaches 0, Δt_e is almost 0. Through eq 6, the transfer from hydration to nonhydration is achieved in a smooth way, and no sudden jump occurs.

To calibrate a general expression for diffusivity (eq 4), large amounts of test data are needed. The experiments should be carried out systematically. By keeping all the parameters constant except one, the effect of that parameter on diffusivity can be checked. This needs to be done for the effects of w/c, concrete composition, temperature, and t_0. The only test data that serve this purpose are those obtained by Molina [23], which will be used in this study. These tests have various w/c values and almost the same t_0 as listed in Table 1. They are labeled 50-03-15, 63-03-15, and 75-03-15, where, for example, the first two digits in 50-03-15 mean $w/c = 0.5$, the next two digits 03 mean $t_0 = 3$ days, and the last two digits 15 mean specimen depth 15 cm. Parrott's drying test results [22], labeled 59-01-10, are also used for parameter calibrations.

The test results used by Bažant and Najjar [1], labeled 66-07-08 and 66-28-08 in Table 1, will not be used here, although a good fit of those test data can be achieved by eq 4 (see Figures 13 and 14). By comparison of those test data with the data shown in Figures 15 to 18, one finds that the trend at small $t - t_0$ (i.e., high relative humidity) is completely different from that in Figures 13 and 14. The old data (Figures 13 and 14) showed a sharp drop of H in both the inner and
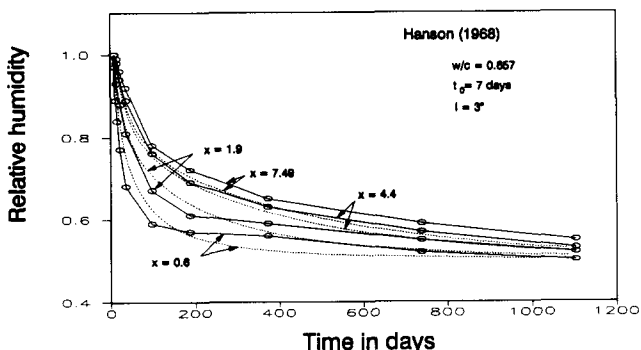

FIGURE 13. Comparison of calculated time dependence of humidity with Hanson's data (1968) for curing period $t_0 = 7$ days.
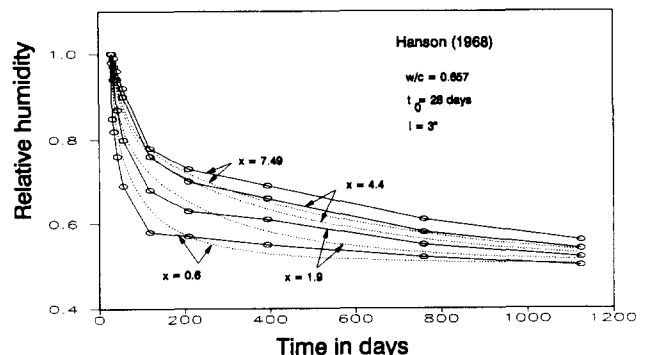

FIGURE 14. Comparison of calculated time dependence of humidity with Hanson's data [24] for curing period $t_0 = 28$ days.
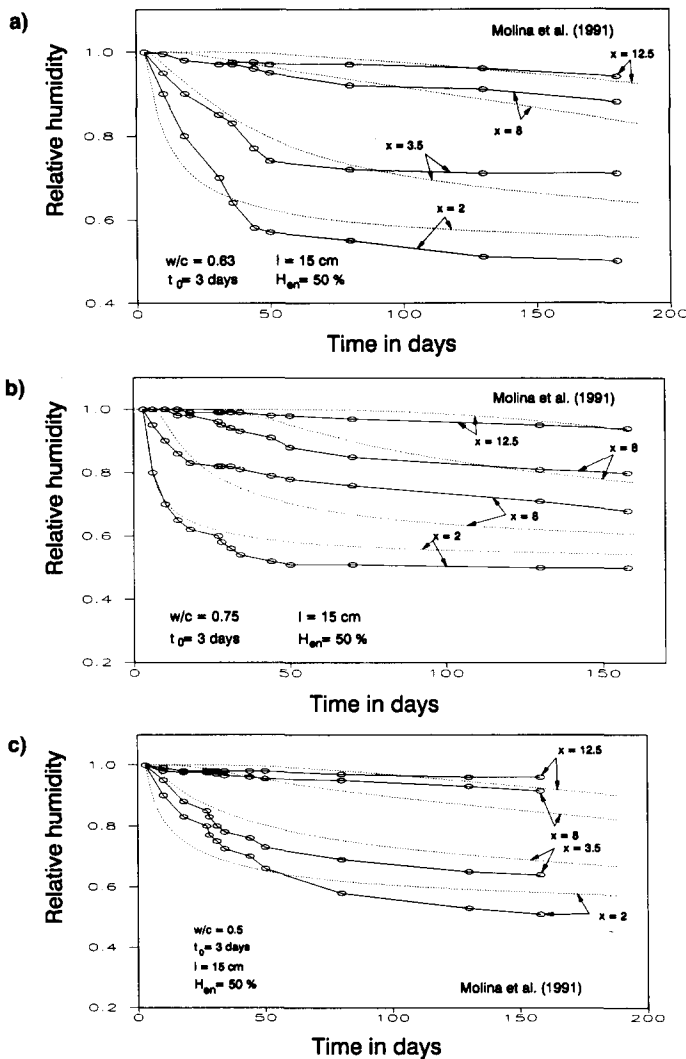
a)

b)

c)

FIGURE 15. Comparisons of calculated time dependence of humidity with Molina's data [23].

$$\alpha_h = 1.05 - 3.8 \frac{w}{c} + 3.56 \left(\frac{w}{c}\right)^2. \tag{7}$$

Upon examination of Figure 10, it is apparent that α_h increases as w/c increases. The optimum curves for β_h and γ_h are:

$$\beta_h = -14.4 + 50.4 \frac{w}{c} - 41.8 \left(\frac{w}{c}\right)^2 \tag{8}$$

$$\gamma_h = 31.3 - 136 \frac{w}{c} + 162 \left(\frac{w}{c}\right)^2. \tag{9}$$

Figures 11 and 12 illustrate eqs 8 and 9. It is apparent that the trends obtained with eqs 7 to 9 agree with those obtained earlier by analysis of the diffusion mechanisms.

The theoretical curves based upon moisture capacity (eq 2) and diffusivity (eqs 4 and 7 through 9) are shown in Figures 13 to 16 in comparison with the test data. All the theoretical curves fit the test curves satisfactorily and give reasonable long-term predictions as well.

Conclusions

1. The moisture capacity, obtained as the derivative of adsorption isotherm, is not a constant. First it drops, then becomes constant, and finally increases. This trend is generally true regardless of the age, type of cement, temperature, and water: cement ratio. The physical meaning of the first turn points in moisture capacity, marking the transition from the initial drop to the constant region at increasing humidity, may correspond to the reaching of monolayer capacity in adsorption isotherm; and the meaning of the second turn point, marking the transition from the constant region to the final increase, may correspond to the beginning of capillary condensation. For
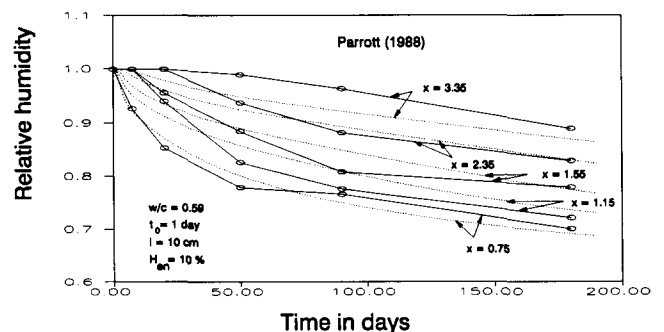
outer layers of the specimens immediately after the exposure, which might not be correct since the inner layer cannot respond that quickly to the change of boundary condition. The recent data (Figures 15 to 16) show the more reasonable trends: the outside layer exhibits a sharp drop of H and the inner layer exhibits a smooth transition from high H to low H. The possible reason for such a difference is that the advanced technique to precisely measure the high relative humidities (80 to 100%) has been developed only during the last 20 years. The parameters α_h, β_h, and γ_h corresponding to the best fit of the old data are not consistent with the values corresponding to the recent results (see Table 1), due to the different trends. Thus, the old data are excluded.

The optimum formula for α_h, illustrated in Figure 10, is

FIGURE 16. Further comparison of calculated time dependence of humidity with Parrott [22].

the usual practical range from 50 to 100%, the moisture capacity keeps increasing with increasing relative humidity.

2. There are three possible diffusion mechanisms for concrete drying: ordinary diffusion, Knudsen diffusion, and surface diffusion. By individual analysis of each diffusion mechanism, the common features of the mechanisms are found: for low humidities, the diffusivities may become constant, and at high humidities, the diffusivities increase, regardless of the mechanism. Therefore, instead of considering combinations of the diffusivities of various mechanisms, a total diffusivity expression that simply reflects these common features is proposed.

3. The improved formula for the dependence of diffusivity on pore humidity, developed herein, gives satisfactory agreement with test data.

4. The influence of the water:cement ratio on the diffusivity is analyzed. With an increasing water:cement ratio, (1) the diffusivity at low humidity level increases; (2) the incremental part of diffusivity increases to a certain point, then decreases, and vanishes asymptotically with a very large water:cement ratio; and (3) the humidity level at which the diffusivity begins increasing becomes higher.

5. The present model for moisture diffusion through concrete gives satisfactory diffusion profiles and correct long-term drying predictions. It is suitable for incorporation in finite element programs for shrinkage and creep effects in concrete structures.

Acknowledgments

References

1. Bažant, Z.P.; Najjar, L.J. Matériaux et Constructions 1972, 5, 3–20.
2. Daian, J.-F. Transport in Porous Media 1988, 3, 563–589.
3. Daian, J.-F. Transport in Porous Media 1989, 4, 1–16.
4. Jonasson, J.-E. Proc. of 8th SMIRT 1985, H5/11, 235–242.
5. Saetta, A.V.; Scotta, R.V.; Vitaliani, R.V. Materials Journal, ACI 1993, 90, 441–451.
6. Bažant, Z.P.; Chern, J.C.; Rosenberg, A.M.; Gaidis, J.M. J. Am. Ceram. Soc. 1988, 71, 776–783.
7. Xi, Y.; Bažant, Z.P.; Jennings, H.M. J. Adv. Cement Based Mater. 1994, 1, 248–257.
8. Mensi, R.; Acker, P.; Attolou, A. Materials and Construction 1988, 21, 3–12.
9. Pihlajavaara, S.E.; Vaisanen, J. Numerical Solution of Diffusion Equation with Diffusivity Concentration Dependent; Publ. No. 87, State Institute for Technical Research, Helsinki.
10. Wittmann, X.; Sadouki, H.; Wittmann, F.H. Proc. of 10th SMIRT 1989, Q, 71–79.
11. Gleysteen, L.F.; Kalousek, G.L. J. Am. Conc. Inst. 1955, 26, 437–446.
12. Hagymassy, J., Jr.; Odler, I.; Yudenfreund, M.; Skalny, J.; Brunauer, S. J. Colloid Interface Sci. 1972, 38, 20–34, 265–276.
13. Mikhail, R.S.; Abo-El-Enein, S.A.; Gabr, N.A. J. Appl. Chem. Biotechnol. 1975, 25, 835–847.
14. Gregg, S.J., Sing, K.S.W. Adsorption, Surface Area and Porosity; Academic Press Inc.: London, 1982.
15. Karger, J.; Ruthven, D.M. Diffusion in Zeolites and Other Microporous Solids; John Wiley & Sons, Inc.: New York, 1992.
16. Bažant, Z.P., Ed. Mathematical Modeling of Creep and Shrinkage of Concrete; John Wiley and Sons: Chichester, 1988.
17. Ruthven, D.M. Principles of Adsorption and Adsorption Processes; John Wiley & Sons, Inc.: New York, 1984.
18. Satterfield, C.N. Mass Transfer in Heterogeneous Catalysis, MIT Press, 1970.
19. Sakata, K. Cement Concrete Res. 1983, 13, 216–224.
20. von Rosenberg, D.U. Methods for the Numerical Solution of Partial Differential Equations; American Elsevier Publishing Company, Inc.: New York, 1969.
21. Powers, T.C. Proc. of the Highway Research Board 1947, 27, 178–188 (PCA Bulletin No. 25).
22. Parrott, L.J. Adv. Cement Res. 1988, 1, 164–170.
23. Molina, L. Private communication on test results obtained at Swedish Cement and Concrete Institute (CBI), Stockholm, 1991.
24. Hanson, J.A. J. Am. Conc. Inst. 1968, 65, 535–543 (also: PCA Bull. D141).